Ultrasonics 94 (2019) 342–349

Contents lists available at ScienceDirect

Ultrasonics

journal homepage: www.elsevier.com/locate/ultras

A practical omni-directional SH wave transducer for structural health monitoring based on two thickness-poled piezoelectric half-rings

Qiang Huan[a,b], Mingtong Chen[a], Faxin Li[a,b,c,*]

[a] LTCS and College of Engineering, Peking University, Beijing 100871, China
[b] Center for Applied Physics and Technology, Peking University, Beijing, China
[c] Beijing Key Laboratory of Magnetoelectric Materials and Devices, Peking University, Beijing, China

ARTICLE INFO

Keywords:
Structural health monitoring
Guided wave
Shear horizontal wave
Omnidirectional
Piezoelectric transducer

ABSTRACT

Structural health monitoring (SHM) has become more and more important in modern industries as it can monitor the safety of structures during the full service life and prevent possible losses of life and economics. Shear horizontal wave in plate-like structures is very useful for long distance inspection since its fundamental mode (SH_0) is totally non-dispersive. However, all the currently available SH wave transducers are not suitable for practical SHM because of their complicated structures. In this work, we firstly investigated via finite element (FEM) simulations the performances of thickness-poled d_{15} PZT ring based omni-directional SH wave piezoelectric transducers (OSH-PT) consisting of different number of elements. Results show that the two-half-ring based OSH-PT can have perfect omni-directivity and acceptable performances in excitation/reception of SH_0 waves. Then, experimental testing on a 21 mm outer-diameter (OD), 9 mm inner-diameter (ID) two-half-ring OSH-PT shows that it exhibits acceptable but not desirable performances in both excitation and reception of SH_0 wave. Finally, size optimization was conducted on the two-half-ring based OSH-PT using FEM simulations and results showed that its performances can be fairly enhanced by reducing the outer diameter of the half-ring. Testing results on a 12 mm-OD, 6 mm-ID OSH-PT show that the SH_0-to-Lamb waves ratio in the case of self-excitation and self-reception can be over 20 dB from 115 kHz to 250 kHz, which is good enough for practical applications. The proposed two-half-ring OSH-PT is expected to be widely used in SH_0 wave based SHM due to its simple structure, easy fabrication/assembling, low cost and good performances.

1. Introduction

Nondestructive testing (NDT) and structural health monitoring (SHM) have been widely used in modern industries as they can evaluate the safety of structures/systems in a nondestructive manner and prevent the possible losses of life and economics [1,2]. The main difference between NDT and SHM is that whether the sensors/probes are movable or fixed on the structures. With the rapid development of wireless sensor technology and computational capacity of personal computers, the applications of SHM turns to be realistic and have been paid more and more attention to in recent years. If it is feasible, SHM is more promising since it can monitor the conditions of structures for the whole service life and remote monitoring is also possible [3]. In a SHM system, sensors or transducers are the most important component, which should be reliable, cost effective, of compact size and easy to assemble.

In the past two decades, guided wave based techniques have been widely used and intensively studied in SHM of large structures [4–8]. Guided waves, e.g., Lamb waves and shear horizontal (SH) waves in plate-like structures, have the advantage of long-distance propagation with small attenuation. So far, Lamb wave based SHM technique have been well investigated in isotropic thin plates and is still under development for layered composites [7]. The rapid development of Lamb wave based SHM is due to the nearly perfect properties of PZT ceramics. A circular thickness-poled PZT wafer is inherently an omni-directional Lamb wave transducer, which is of high signal to noise ratio (SNR), cost effective, small and easy to be bonded on plates. However, Lamb waves are inherently dispersive, of multi-mode and encounter mode conversions at defects or boundaries, introducing difficulties in explanation of the received signals. Giurgiutiu proposed that quasi-single mode Lamb wave can be excited by frequency tuning [9]. However, at the tuned frequency, the quasi-single mode Lamb wave may still be dispersive. Furthermore, in practical SHM applications, many PZT wafers are required and it is not possible to ensure that all the wafers have the best

* Corresponding author at: LTCS and College of Engineering, Peking University, Beijing 100871, China.
E-mail address: lifaxin@pku.edu.cn (F. Li).

https://doi.org/10.1016/j.ultras.2018.07.010
Received 23 April 2018; Received in revised form 27 June 2018; Accepted 18 July 2018
Available online 19 July 2018
0041-624X/

tuning properties at a single frequency. Therefore, in Lamb wave based SHM systems, it is rather difficult to achieve a high SNR in defect imaging [10,11].

In comparison, the fundamental SH wave (SH_0) is totally non-dispersive and less mode conversion will occur when it encounters defects or boundaries. However, it is not straightforward to excite SH_0 wave in plates. Traditionally, SH_0 waves can be excited by using electromagnetic acoustic transducers (EMAT) in a non-contact manner which was firstly introduced by Thompson in late 1970s [12]. Later, the magnetostrictive patch transducers (MPT) were developed and had been used in pipe inspection since the coupling efficiency of MPT is much higher than that of EMAT [13–15], and the fundamental torsional wave T(0,1) in pipes is analogous to SH_0 in plates, i.e., both are non-dispersive [16]. T(0,1) wave can also be excited/received by a thickness-shear (d_{15}) PZT based piezoelectric ring in a dry-coupled manner or bonded on the pipe [17–19]. However, a d_{15} PZT wafer not only generates SH_0 waves, but also generates Lamb waves in plates simultaneously [20,21]. Recent investigations indicate that SH_0 wave can also be excited by using d_{36} face-shear piezoelectric crystals and ceramics [22,23]. But single mode SH_0 wave still cannot be excited until the recent narrow-band SH_0 wave excitation by using synthetic d_{36} mode PZT wafers [24,25]. Miao et al proposed a new face-shear d_{24} mode in PZT wafers and successfully excited single-mode SH_0 wave in a wide frequency range [26]. Furthermore, the d_{24} mode PZT wafer can filter Lamb waves and receive SH_0 wave only in a wide frequency range. The d_{24} mode PZT wafers was also assembled into a ring to excite and receive T(0,1) wave in pipes [27]. Recently, Koehler et al. proposed an SH wave piezoelectric fiber patch transducers (SH-PFP) based on the principle of synthetic deformation [28].

It should be noted that all the above-mentioned SH wave transducer are directional and cannot be directly used for SHM applications where omni-directional transducers are required. Omni-directional SH wave transducers were firstly realized by Kim et al using MPT [29] and later using EMAT [30]. Recently, Liu et al employed the MPT based omni-directional SH_0 wave transducer array to detect defects in quasi-isotropic composites [31]. However, due to the complicated structures and high power driving problem, both the omni-directional MPT and EMAT are not suitable for SHM applications. Borigo et al proposed a design of omni-directional SH wave piezoelectric transducer (OSH-PT) based on two circumferentially poled PZT half-rings [32]. However, although some PZT manufacturers claimed so, uniform circumferential polarization cannot be possibly realized in a half-ring because the induced polarization during poling is not proportional to the applied field. In practice, quasi-uniform circumferential polarization is usually synthesized by assembling several in-plane poled PZT elements circumferentially, such as the Langevin torsional transducers [33]. Belanger and Boivin fabricated an OSH-PT by synthesizing circumferential polarization using six d_{15} mode PZT wafers [34]. The sensitivity deviation in omni-directionally generating SH_0 waves is around 20% while the reception properties were not examined. Miao et al built an OSH-PT based on synthesized circumferential polarization using twelve d_{24} mode PZT wafers [35]. The omni-directional sensitivity deviations in SH_0 wave generation and reception are both around 15%. It should be noted that uniform circumferential polarization is rather difficult to be synthesized because it is almost impossible to ensure that the polarization in each PZT wafer is exactly the same, although the size can be strictly controlled. Recently, Huan et al proposed an OSH-PT based on a thickness-poled, thickness-shear (d_{15}) PZT ring in which the electric field is applied circumferentially by evenly dividing the ring into twelve wafers [36]. Thanks to the uniform thickness-polarization in each wafers, the omni-directional sensitivity deviations in generating and receiving SH_0 waves are only 6–7%. The thickness-poled d_{15} PZT ring based OSH-PTs have shown superior performances in defect imaging and localization, compared to the Lamb wave counterparts [37]. However, this OSH-PT still consists of twelve PZT elements and is not easy to fabricate/assemble, which is not suitable for practical SHM applications where usually a large number of transducers are required to be fixed on the structures.

In this work, we aimed to develop an OSH-PT for practical SHM applications which should be easily fabricated and assembled on structures. The primary candidate is the thickness-poled d_{15} PZT ring equally dividing into several elements. Firstly, finite element (FEM) simulations were conducted to examine the performances of the thickness-poled d_{15} PZT ring with different number of elements in excitation and reception of SH_0 waves. Results show that an OSH-PT consisting of two thickness-poled PZT half-rings can have uniform sensitivity along all directions. Then, an OSH-PT based on two half-rings with the OD of 21 mm, ID of 9 mm was fabricated and its performances were systematically tested. Results show that this OSH-PT can excite and receive SH_0 wave with SH_0-to-Lamb waves ratio (SLR) about 15 dB in a wide frequency range, which is acceptable but not desirable. Finally, size optimization was performed on the half-ring OSH-PT using both FEM simulations and experiments. Testing results on a 12 mm-OD, 6 mm-ID OSH-PT show that the SLR in the case of self-excitation and self-reception is above 20 dB in a wide frequency range, which is good enough for practical applications. The proposed two-half-ring OSH-PT is very easy to fabricate and assemble, which is expected to pave the way to practical SHM systems based on SH waves.

2. Transducer design and finite element simulations

2.1. Design of a practical omni-directional SH wave piezoelectric transducer (OSH-PT)

The primary candidate for the practical OSH-PT is the thickness-poled d_{15} mode PZT ring since such a ring consisting of twelve elements had been verified to have very good performances in excitation/reception of SH_0 wave omni-directionally [36]. Since a ring with twelve elements is not easy to fabricate or assemble, we want to examine the performances of such a ring with fewer elements If its performance is acceptable, then it can turn to be a practical OSH-PT for SHM applications. Fig. 1 shows the design of an OSH-PT based on thickness-poled

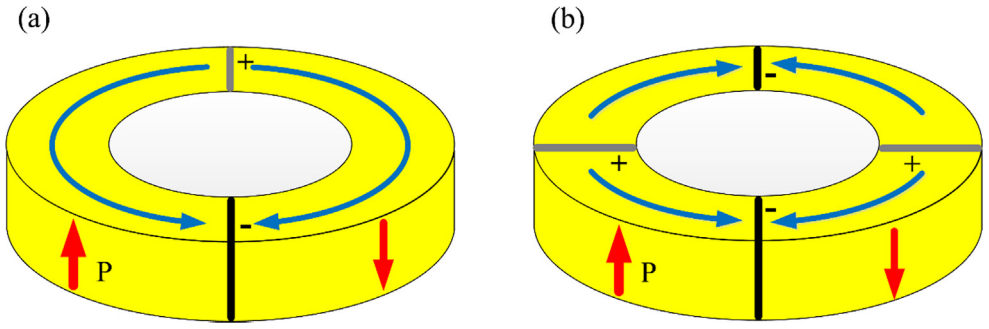

Fig. 1. Design of practical OSH-PT based on thickness-poled d_{15} mode PZT rings with few elements: (a) two half-rings; (b) four quarter-rings.

d_{15} mode PZT rings consisting of two half-rings and four quarter-rings. The PZT ring is firstly poled along the thickness direction which is easy to realize. After poling, the ring is cut into even-number elements along its diameter. Then the top/bottom electrodes were removed and lateral electrodes were spread for circumferential field loading. In assembling the OSH-PT, the poling directions of the adjacent elements were opposite thus they can share the common lateral electrodes.

2.2. Finite element simulation procedures

Firstly, finite element (FEM) simulations were carried out in ANSYS to check the performances of OSH-PT based on thickness-poled d_{15} mode PZT rings with different number of elements in excitation and reception of SH_0 waves. An aluminum plate (with the Young's modulus of 69 GPa, Poisson ratio of 0.33, and density of 2700 $kg{\cdot}m^{-3}$) was modeled by element SOLID 185 with the dimensions of 400 mm × 400 mm × 2 mm. The OSH-PT modeled by elements SOLID 5 was bonded on the central of the plate, and its material was PZT-5H whose properties can be found elsewhere [38]. For comparison, the dimensions of the ring are firstly fixed to be the same as that in previous studies [36] (with the outer diameter (OD) of 21 mm, inner diameter (ID) of 9 mm and thickness of 2 mm). During the simulations, the excitation signal was modulated into a five cycle sinusoid tone burst enclosed in Hanning window with central frequency of 180 kHz. The drive voltage was set to be inversely proportional to the number of elements thus to keep the same electric field intensity for all the cases. For the two half-ring case, the drive voltage is 120 V.

2.3. FEM simulation results

The performances of the thickness poled d_{15} mode PZT rings consisting of 2, 4, 6, 8, 10, 12 and 16 elements in excitation of SH_0 wave is firstly simulated. Due to the limited space, only the results for the 2 (half-rings), 8 and 12 elements cases were plotted in Fig. 2. Firstly, the tangential displacement dominated by SH_0 wave were compared for these three cases. The snapshots of the displacement fields at 50 μs were shown in Fig. 2(a), (b), and (c). It can be found that all the three tangential displacement fields were perfectly axisymmetric, which means that SH_0 wave were generated omni-directionally with uniform amplitudes. The amplitude of SH_0 wave for these three cases is very close to each other. It slightly decreases with the increasing number of elements, which should be due to the reduced in-plane stiffness of the whole ring. When comparing the total displacement components in time-domain, the results were quite different, as seen in the bottom row of Fig. 2. Besides the SH_0 wave (u_y), the S_0 wave (radial displacement component u_x) and A_0 wave (out-of-plane displacement component u_z) also appeared and A_0 is always dominant to S_0 for all these three cases. Meanwhile, it can be seen that the amplitudes of Lamb waves decrease with the increasing number of elements. This indicates that Lamb waves (A_0 wave in this work) can be better suppressed in an OSH-PT consisting of more elements where the out-of-plane stiffness of each element is fairly considerably enhanced.

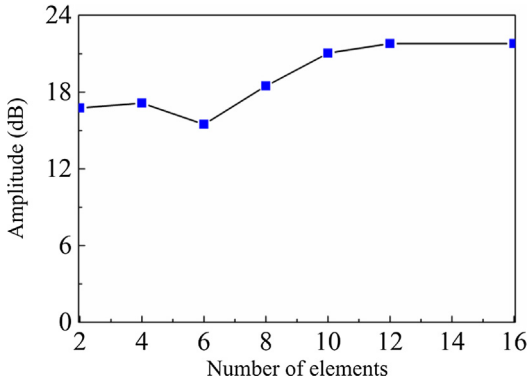

Fig. 3. The simulated ratio of the excited SH_0 wave to Lamb waves ratio by the 21 mm-OD OSH-PTs consisting of different number of elements.

Fig. 3 presented the simulated SLR of the excited SH_0 wave by the OSH-PT consisting of different number of elements. It can be seen that overall the SLR increases with the increasing number of elements, it is about 16.5 dB for the two-half-ring case and saturates at about 22 dB when the element number is over twelve. However, there is an

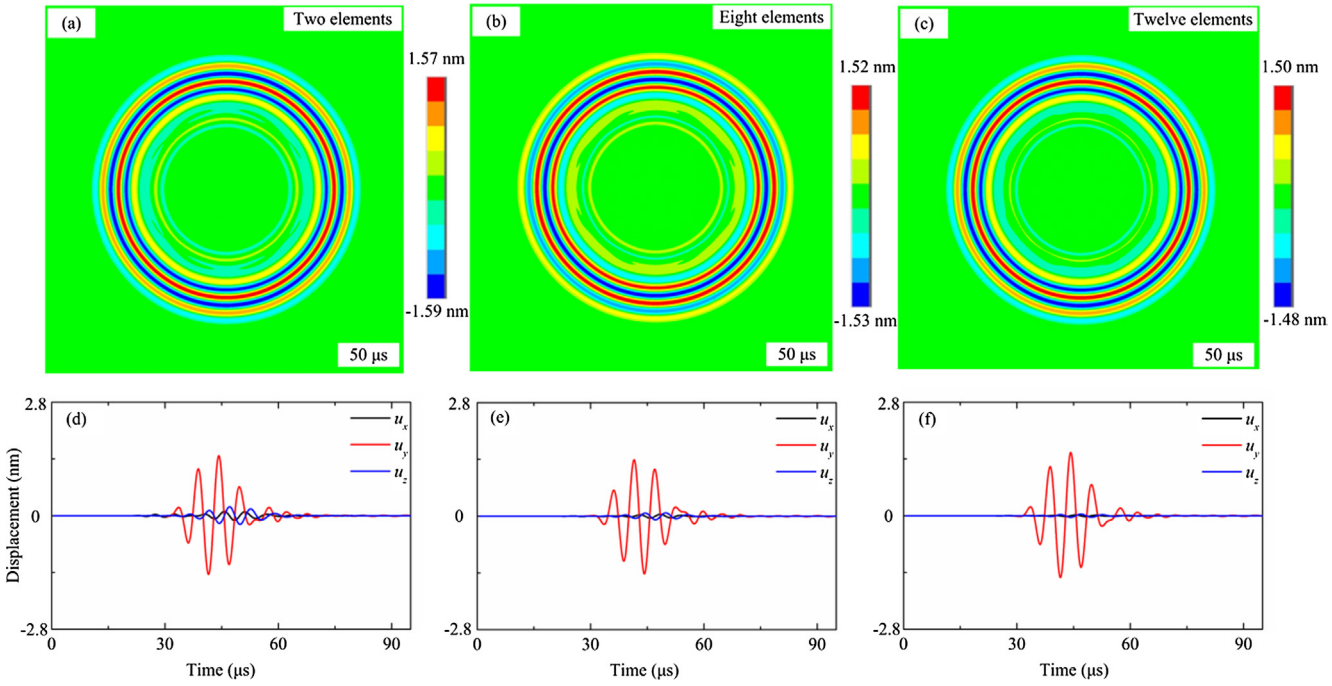

Fig. 2. FEM simulations results on the 21 mm-OD OSH-PTs consisting of different number of elements in SH_0 wave excitation. (Up): transient tangential displacement component at 50 μs; (Bottom): Time-domain displacement components under cylindrical coordinates. (Left): Two elements; (Middle): eight elements; Right): Twelve elements.

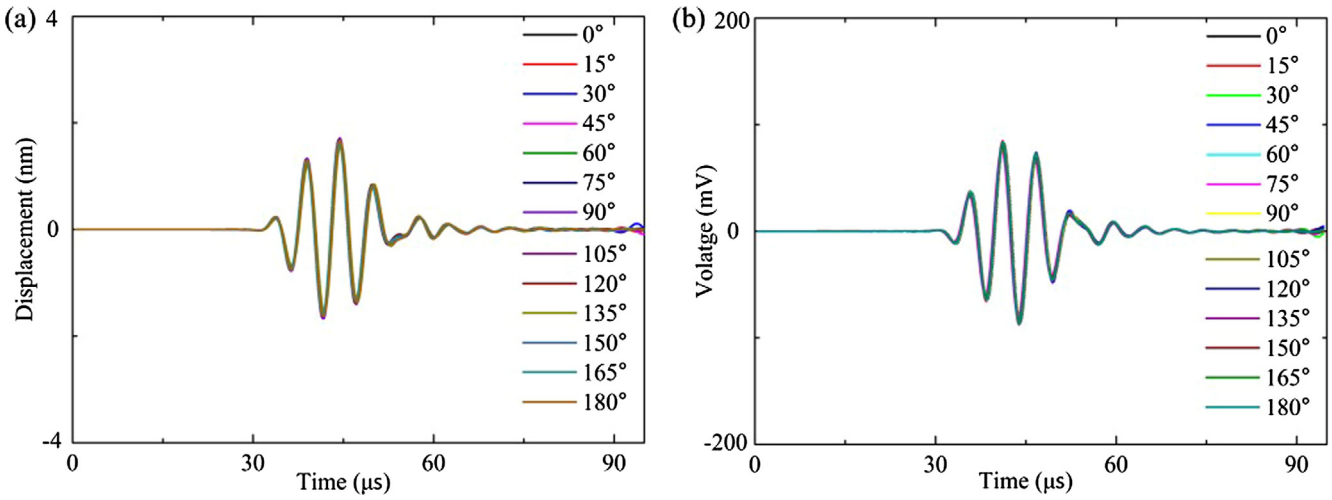

Fig. 4. Time-domain FEM simulation results of the two-half-ring OSH-PT in exciting and receiving SH_0 wave. (a) Tangential displacement excited by the OSH-PT at different directions; (b) voltage signals received by the OSH-PT at different directions.

exception for the six-element case whose SLR in excitation is only about 15 dB, even lower than that for the two and four-elements case. The mechanism for this exception cannot be well clarified at present, while this may explain the reported poor SLR in excitation of SH_0 wave by using an OSH-PT consisting of six d_{15} PZT elements [34].

Since the simulated SLR in SH_0 wave excitation by the two-element (two-half-ring) OSH-PT is very close to that by the four-element case, the two-half-ring OSH-PT is thus further investigated since it is the most convenient for fabrication and assembling. To further examine the omni-directional excitation/reception performances of the two-half-ring OSH-PT, time-domain FEM simulations were carried out in ANSYS. Centering at the OSH-PT, thirteen monitoring points were positioned at a 100 mm-radium circle with the angle interval of 15°. When checking its performance in SH_0 wave generation, tangential displacements were picked up at the monitoring points. The results were shown in Fig. 4(a). It can be seen that all signals along different directions were entirely overlapped, which further conformed the uniform omni-directivity of the OSH-PT in SH_0 wave generation. Meanwhile, the waveform of the received signals was the same as that of the input signal with little distortion. When checking the two-half-ring OSH-PT's performance in SH_0 wave reception, tangential displacements were applied at the monitoring points respectively to simulate the SH_0 wave and the OSH-PT served as a sensor. The received voltages were shown in Fig. 4(b). Again, all signals were totally overlapped without waveform distortion. These results indicated that theoretically the two-half-ring OSH-PT can generate and receive SH_0 wave omni-directionally with uniform sensitivity.

3. Experiments on the 21 mm-OD, 9 mm-ID, 2 mm-thick two-half-ring OSH-PT

Since the FEM simulation results show that the OSH-PT consisting of two half-rings can generate SH_0 wave with the SLR better than 16 dB and the omni-directivity is theoretically perfect, we then fabricated the two-half-ring OSH-PT and examined its performances experimentally. The size of the tested OSH-PT here is the same as what reported previously for comparison [37] (21 mm-OD, 9 mm-ID and 2 mm-thick). The layout of the testing setup for SH_0 wave excitation and reception was shown in Fig. 5. During testing, the two-half-ring OSH-PT and d_{36} type PMN-PT wafers (which can excite/receive both SH_0 wave and Lamb waves) were directly glued (without additional constraints) onto a 1000 mm × 1000 mm × 2 mm aluminum plate as actuator/sensors with the distances of 360 mm. A five-cycle Hanning window-modulated sinusoid signal generated by a functional generator (Agilent 33220A) and amplified by a power amplifier (KH7602M) was used to drive the actuator. A digital oscilloscope (Agilent DSO-X 3024A) was used to collect the wave signals received by the sensors. In all the testing, the drive voltage for the two-half-ring OSH-PT is 120 V and that for the d_{36} type PMN-PT wafer is 50 V.

Firstly, the performance of the two-half-ring OSH-PT in excitation of SH_0 wave is examined by using the 21 mm-OD OSH-PT as the actuator and a d_{36} type PMN-PT crystal as the sensor. Fig. 6 shows the wave signals excited by the OSH-PT and received by the PMN-PT crystal at 180 kHz along the 0° direction. There is only one wave package in the received signal. By continuous wavelet transform (CWT) of the drive and received signals, the propagation time of the wave mode is determined to be 115.5 μs and the group velocity is calculated to be 3116 $m{\cdot}s^{-1}$, which is very close to the theoretical velocity of SH_0 wave in aluminum plate (3099 $m{\cdot}s^{-1}$). Since the PMN-PT wafer can receive both SH_0 wave and Lamb waves, and there is no other wave mode in the received signal in Fig. 6(a), we can conclude that the two-half-ring OSH-PT can excite single mode SH_0 wave at 180 kHz.

The frequency dependent performances of the 21 mm-OD two-half-ring OSH-PT in generation and reception of SH waves were systematically examined by using the OSH-PT as the actuator (sensor) and the d_{36} type PMN-PT crystal as the sensor (actuator) which can excite/receive both SH_0 wave and Lamb waves. The testing results were plotted in Fig. 7. It can be seen that the OSH-PT can excite single mode SH_0 wave in a wide frequency range from 100 kHz to 250 kHz. The SLR of the excited SH_0 wave can reach over about 16 dB. When the OSH-PT serves as a sensor, it can filter some of the generated Lamb waves and receive the SH_0 wave in a wide frequency range. Since both the receiving and actuating properties of the PMN-PT wafer are frequency dependent [22], the results in Fig. 7 cannot accurately represent the frequency-dependent excitation/reception performances of the two-half-ring OSH-PT.

Fig. 8 shows the omni-directivity of the 21 mm-OD two-half-ring OSH-PT in generation and reception of SH_0 wave at 180 kHz where the amplitude is normalized with regard to the average amplitude. It can be seen that the omni-directivity of the two-half-ring is quite good in both excitation and reception with the maximum deviation error of ~14%. Since the FEM simulation results had indicated that the theoretical omni-directivity of this OSH-PT is perfect, the deviation errors should not come from the transducer design, but from the variations in properties of different PMN-PT wafers, bonding conditions of the actuators and sensors, etc.

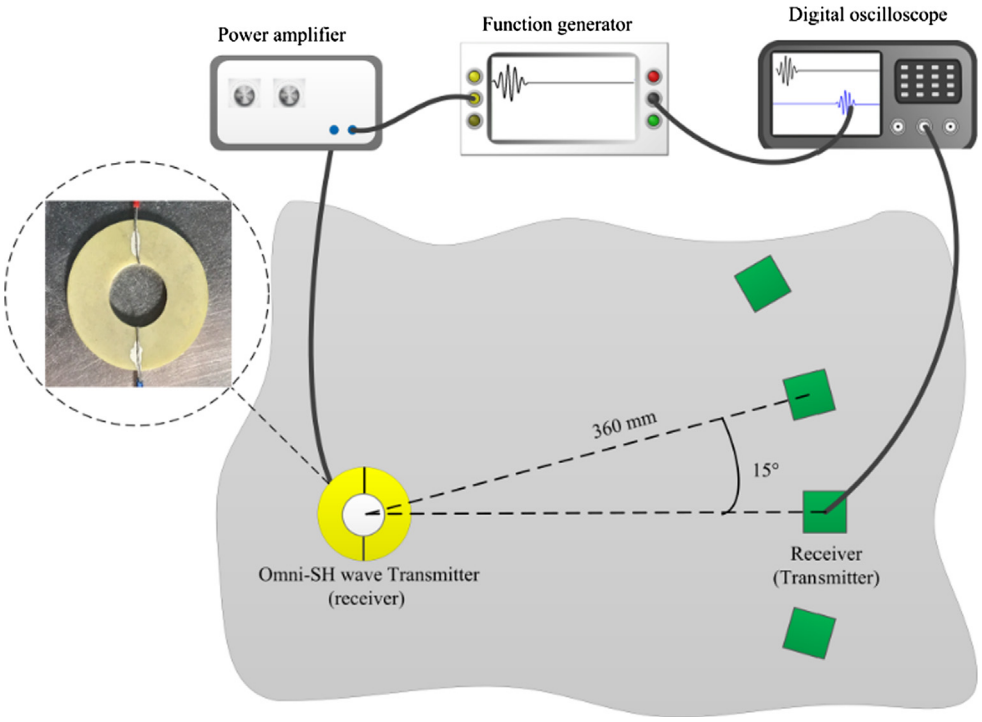

Fig. 5. The schematic of testing setup to check the excited/received wave mode and omni-directivity of the two-half-ring OSH-PT.

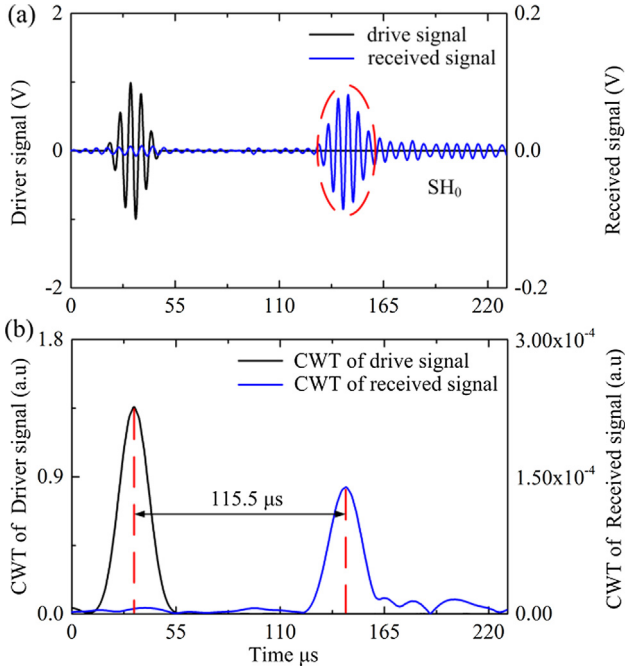

Fig. 6. (a) Signals excited by the 21 mm-OD two-half-ring OSH-PT at 180 kHz with drive voltage of 120 V and received by a d_{36} type PMN-PT single crystal wafer. (b) Continuous wavelet transform (CWT) of the drive signal and received signal.

4. Size optimization of the two-half-ring based OSH-PT

Since the FEM simulations results in Fig. 2(d) had indicated that in SH wave excitation using the 21 mm-OD two-half-ring OSH-PT, the Lamb waves cannot be completely suppressed, we further conducted size optimization on the two-half-ring OSH-PT using FEM simulations for possible improvement. Firstly, with the fixed thickness of 2 mm, the outer diameter and outer to inner diameter ratio of two-half-ring OSH-PTs were optimized and the simulated SLR was shown in Fig. 9(a). It can be seen that overall the SLR increases steadily with the decreasing outer diameter, i.e., the Lamb waves were better suppressed in the case of small ring. This may be due to the fact that decreasing the ring size had enhanced the out-of-plane bending stiffness of the half-ring, suppressing the excited out-of-plane wave mode (A_0). In comparison, the outer to inner diameter ratio has little influence on the SLR of the excited SH_0 wave, except for the cases when the outer diameter is around 15 mm or 20 mm and the ratio is around 2.0. In Fig. 9(a), the circled zone was the optimized OSH-PT with the SLR over 22 dB. The optimized OD and outer to inner diameter ratio were around 12 mm and 2, respectively. Then, the thickness dependence of the SLR were simulated using four OD/ID pairs and the results were shown in Fig. 9(b). It can be seen that within the range from 1 mm to 3 mm, the SLR of the OSH-PT was insensitive to thickness. Furthermore, for all the simulated OD/ID pairs, the SLR reaches its maxima at the thickness of 2 mm. It should be noted for a PZT ring, the smaller the OD and ID is, the more difficult it would be in fabrication. An OSH-PT with the OD of 8 mm and ID of 4 mm is rather difficult to fabricate. Taking all these factors into account, the OSH-PT with the OD of 12 mm, ID of 6 mm and thickness of 2 mm may be a desirable choice in practical applications.

Based on the size optimization results in Fig. 9, we further fabricated several two-half-ring OSH-PTs with another two sets of dimensions: OD-ID of 16 mm-8 mm and 12 mm-6 mm, and the thickness remains at 2 mm. Furthermore, to examine the performances of the two-half-ring OSH-PTs in practical testing, the wave signals obtained from three actuator/sensor pairs including d_{24} PZT/OSH-PT, OSH-PT/d_{24} PZT and OSH-PT/OSH-PT were measured for different-size OSH-PTs. The former two actuator/sensor pairs can be used in tomography applications [39] and the OSH-PT/OSH-PT pair is applicable to all the monitoring cases. In the testing, the in-plane poled d_{24} PZT wafer is 8 mm × 8 mm × 1 mm in dimension and electric field is applied/received in another in-plane direction. For all the testing, the drive voltage is fixed at 120 V and the results at 180 kHz were shown in Fig. 10. It can be seen from the top row that for all the three actuator/sensor pairs, the unwanted wave (or noise) other than the SH_0 mode is obvious for the 21 mm-9 mm (OD-ID) OSH-PT case, which is consistent with the

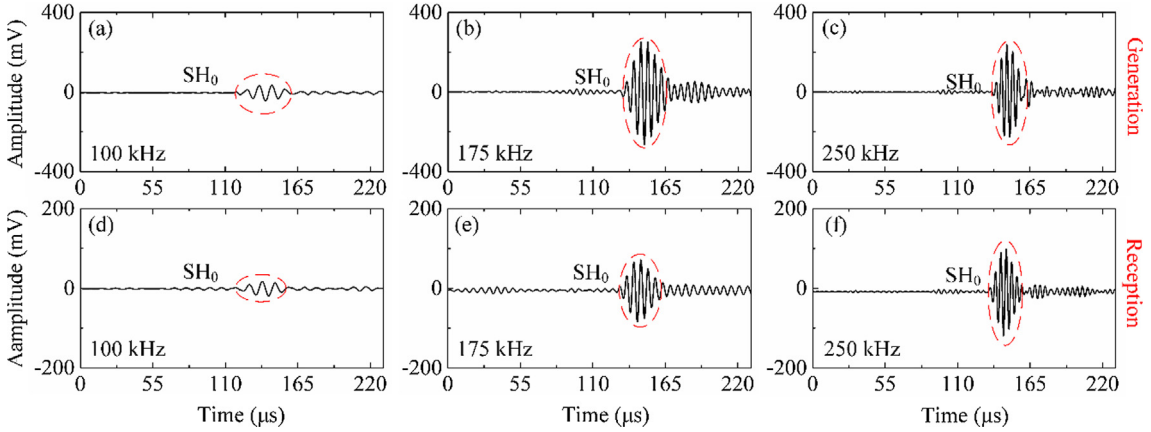

Fig. 7. (up) Frequency dependent wave signals excited by the 21 mm-9 mm two-half-ring OSH-PT with drive voltage of 120 V and received by a d_{36} type PMN-PT wafer; (bottom) Frequency dependent wave signals excited by a d_{36} type PMN-PT wafer with drive voltage of 50 V and received by the two-half-ring OSH-PT.

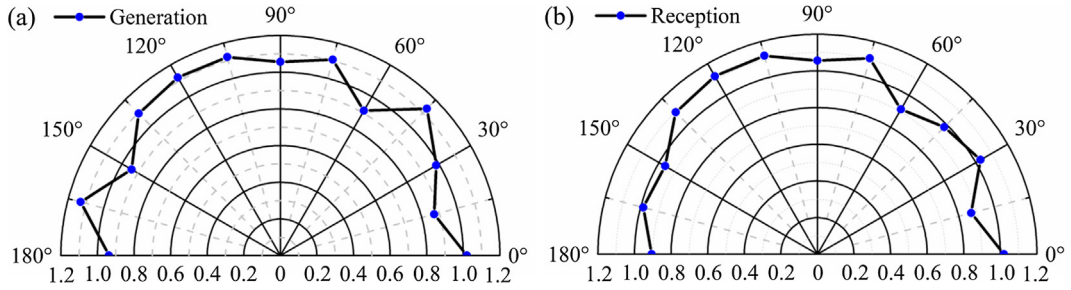

Fig. 8. The omni-directivity of the 21 mm-OD two-half-ring OSH-PT in (a) generation and (b) reception of SH_0 wave at 180 kHz. Wave signals were excited/received by the OSH-PT and d_{36} type PMN-PT single crystal wafers. The amplitude is normalized by the average amplitude.

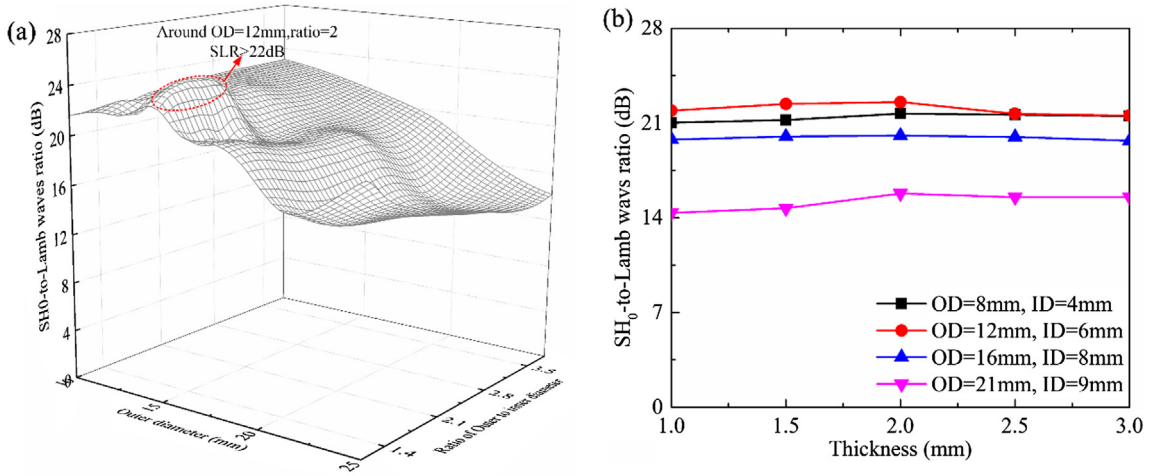

Fig. 9. The simulated SLR in SH_0 wave excitation using different-sized two-half-ring OSH-PTs: (a) fixed thickness of 2 mm, varied outer diameters and outer to inner diameter ratios; (b) thickness dependence for different OD/IDs.

FEM simulation results in Fig. 2(d). In comparison, for both the 16 mm-8 mm OSH-PT and 12 mm-6 mm OSH-PT cases, the amplitudes of the unwanted wave modes were significantly reduced, as seen in the middle and bottom rows of Fig. 10.

To further examine the validity of the optimization process using FEM simulations, comparisons between the simulations and experimental testing was made for the above three OSH-PTs and the results were shown in Fig. 11. It can be seen from Fig. 11(a) that with the increase of the outer diameter, the SLR of the OSH-PTs decreased steadily both in simulations and experiments. Although the simulated values of SLR cannot match the testing results very well, the similar tendencies for the simulations and experiments can reveal the positive correlation between them. The observed higher SLR of the simulations is easy to understand. The FEM simulations was carried out in ideal boundary conditions, problems such as the non-uniform bonding and fabrication errors will not appear. However, these factors do exist in practical testing, which resulted in the decreased SLR. Thus, the experimental SLR is always lower than the simulated SLR. Fig. 11(b), (c) and (d) listed typical wave signals generated by the 2 mm-thick OSH-PTs with the OD-ID of 12 mm-6 mm,16 mm-8 mm, 21 mm-9 mm and received by a d_{36} type PMN-PT wafer at 180 kHz, respectively. It can be seen that with the increase of the outer diameter, the amplitude of the received unwanted wave modes become higher, leading to the lower SLR of the large-sized OSH-PT.

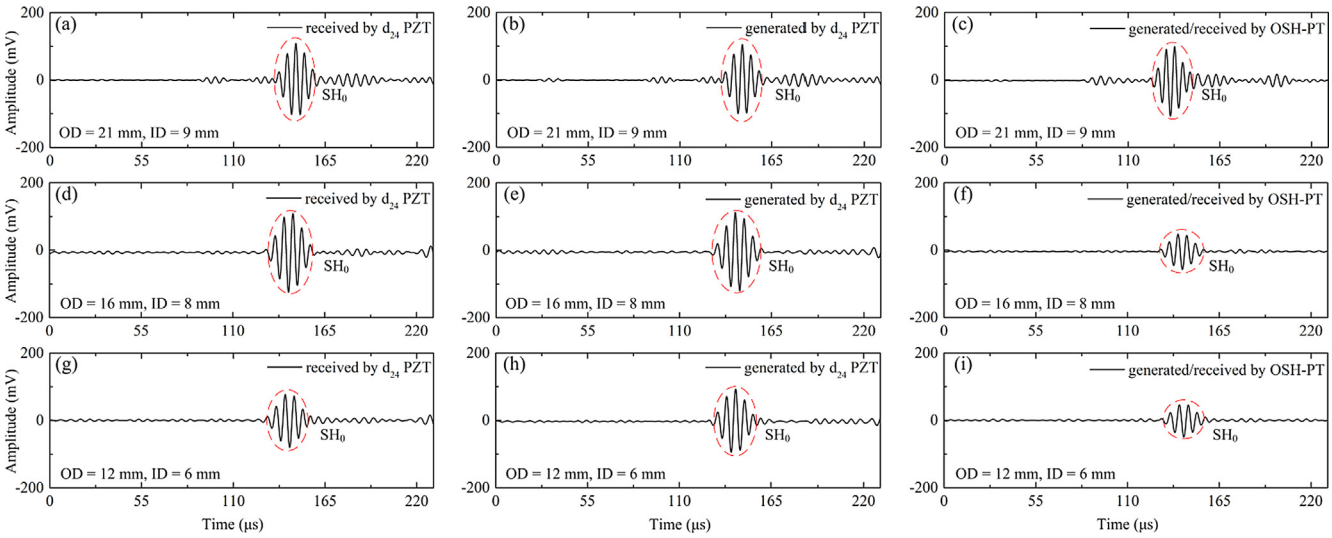

Fig. 10. The received SH_0 wave signals from different actuator/sensor pairs for different-sized OSH-PT at 180 kHz. Left column: d_{24} PZT/OSH-PT; Middle Column: OSH-PT/d_{24} PZT; Right Column: OSH-PT/OSH-PT. Up row: 21 mm-OD, 9 mm-ID; Middle row: 16 mm-OD, 8 mm-ID; Bottom row: 12 mm-OD, 6 mm-ID.

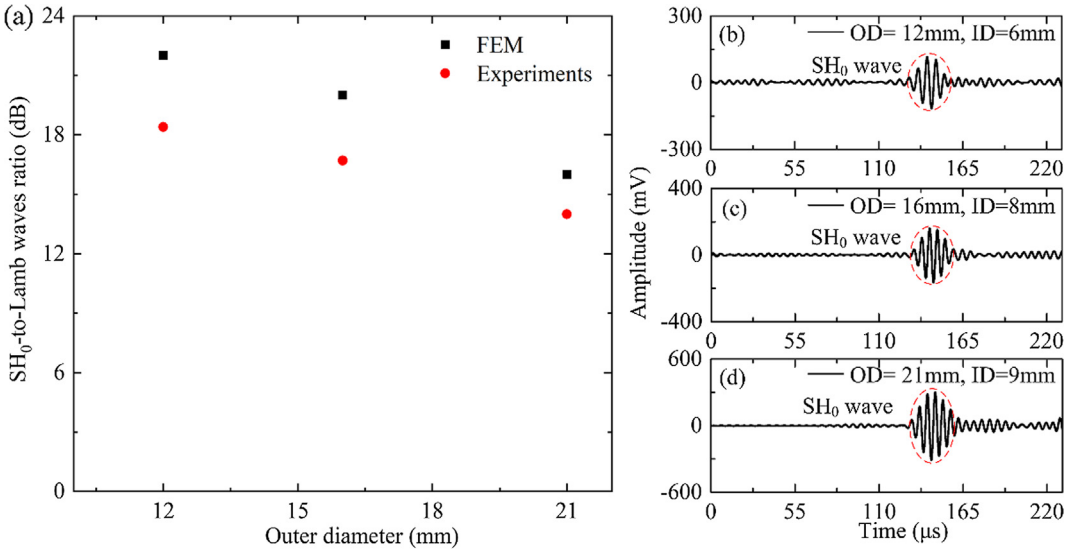

Fig. 11. (a) The comparisons between the FEM simulations and experimental results on SH_0-to-Lamb waves ratio (SLR) for 2 mm-thick OSH-PTs with different OD/IDs. Wave signals generated by an OSH-PT with the OD-ID of (b) 12 mm-6 mm, (c) 16 mm-8 mm, and (d) 21 mm-9 mm and received by d_{36} PMN-PT wafer at 180 kHz, respectively.

The SLR of the received wave signals during self-excitation/self-reception for different-sized OSH-PTs were further measured from 100 kHz to 250 kHz and the results were shown in Fig. 12. The SLR of the twelve-element OSH-PT [36] was also plotted for comparison. It can be seen that the SLRs for the 21 mm-9 mm (OD-ID) two-half-ring OSH-PT is below 16 dB for most frequencies. The SLRs for the 16 mm-8 mm OSH-PT is higher, which is above 17 dB for most frequencies and can be above 20 dB in a narrow frequency range from 170 kHz to 195 kHz. The 12 mm-6 mm OSH-PT performed the best. Its SLR can be above 20 dB in a wide frequency range from 115 kHz to 250 kHz and can even reach 25 dB in a narrow band from 125 kHz to 145 kHz, which is good enough for practical applications [17].

In Fig. 12, when comparing the performances of the optimized 12 mm-6 mm two-half-ring OSH-PT in this work with the twelve-element OSH-PT reported previously [36], it is found that although generally the SLR of the former is slightly smaller than that of the latter, in some frequencies the former is even better than the latter. That is, the optimized two-half-ring OSH-PT simplifies the transducer structure while keeps the good performances, which is very promising in practical SHM applications where a large number of transducers are required.

5. Conclusions

In summary, we firstly demonstrated via FEM simulations that OSH-PTs based on two thickness poled d_{15} PZT half-rings can all show uniform omni-directivity in SH_0 wave excitation and reception. Then, the two-half-ring OSH-PT with the outer-diameter of 21 mm and inner diameter of 9 mm was fabricated and its performances were systematically examined. Results show that its omni-directivity is fairly good with the maximum deviation of 14%, which should be mainly caused by the fabrications and measurement limitations. The SLR of the 21 mm-9 mm two-half-ring OSH-PT in SH wave excitation/reception can reach about 15 dB, which is acceptable but not desirable. Finally, size optimization was conducted on the two-half-ring OSH-PT using FEM simulations. The SLR of the OSH-PT increases steadily with the decreasing outer diameter. Experimental testing on a 12 mm-OD, 6 mm-ID two-half-ring OSH-PT shows that the SLR in the case of self-

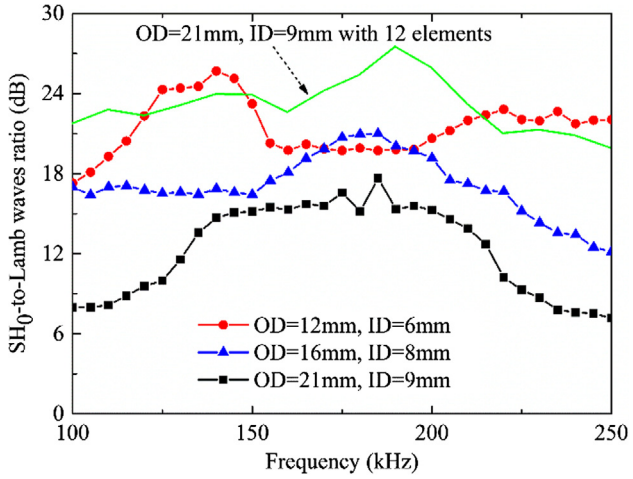

Fig. 12. Frequency dependent SLR of the received wave signals during self-excitation/self-reception for different sized two-half-ring OSH-PTs. The SLR of the twelve-element OSH-PT [36] was also plotted for comparison.

excitation and self-reception can reach above 20 dB in a wide frequency range, which is good enough for practical applications. The proposed two-half-ring OSH-PT in this work is expected to pave the road to wide applications of SH wave based SHM.

Acknowledgements

This work is supported by the National Natural Science Foundation of China under Grant Nos. 11672003 and 11521202.

References

[1] R. Halmshaw, Non-destructive testing, Arnold, 1991.
[2] D. Balageas, C.-P. Fritzen, A. Güemes, Structural health monitoring, John Wiley & Sons, 2010.
[3] J.P. Lynch, K.J. Loh, A summary review of wireless sensors and sensor networks for structural health monitoring, Shock Vib. Dig. 38 (2006) 91–130.
[4] A. Raghavan, C.E. Cesnik, Review of guided-wave structural health monitoring, Shock Vib. Dig. 39 (2007) 91–116.
[5] Z. Su, L. Ye, Y. Lu, Guided Lamb waves for identification of damage in composite structures: a review, J. Sound Vib. 295 (2006) 753–780.
[6] W.J. Staszewski, Structural health monitoring using guided ultrasonic waves, Adv. Smart Technol. Struct. Eng. Springer, 2004, pp. 117–162.
[7] J.-B. Ihn, F.-K. Chang, Pitch-catch active sensing methods in structural health monitoring for aircraft structures, Struct. Health Monit. 7 (2008) 5–19.
[8] V. Giurgiutiu, Structural health monitoring: with piezoelectric wafer active sensors, Academic Press, 2007.
[9] V. Giurgiutiu, Tuned Lamb wave excitation and detection with piezoelectric wafer active sensors for structural health monitoring, J. Intell. Mater. Syst. Struct. 16 (2005) 291–305.
[10] L. Yu, V. Giurgiutiu, In situ 2-D piezoelectric wafer active sensors arrays for guided wave damage detection, Ultrasonics 48 (2008) 117–134.
[11] J.E. Michaels, Detection, localization and characterization of damage in plates with an in situ array of spatially distributed ultrasonic sensors, Smart Mater. Struct. 17 (2008) 035035.
[12] C. Vasile, R. Thompson, Excitation of horizontally polarized shear elastic waves by electromagnetic transducers with periodic permanent magnets, J. Appl. Phys. 50 (1979) 2583–2588.
[13] R.B. Thompson, Generation of horizontally polarized shear waves in ferromagnetic materials using magnetostrictively coupled meander-coil electromagnetic transducers, Appl. Phys. Lett. 34 (1979) 175–177.
[14] H. Kwun, S. Kim, J.F. Crane, Method and apparatus generating and detecting torsional wave inspection of pipes or tubes, U.S. Patent 6,917,196, (2002).
[15] I.K. Kim, Y.Y. Kim, Wireless frequency-tuned generation and measurement of torsional waves using magnetostrictive nickel gratings in cylinders, Sens. Actuat. Phys. 126 (2006) 73–77.
[16] J.L. Rose, Ultrasonic guided waves in solid media, Cambridge University Press, 2014.
[17] D. Alleyne, B. Pavlakovic, M. Lowe, P. Cawley, Rapid, long range inspection of chemical plant pipework using guided waves, Trans. Tech. Publ. (2004) 434–441.
[18] P. Cawley, M. Lowe, D. Alleyne, B. Pavlakovic, P. Wilcox, Practical long range guided wave inspection-applications to pipes and rail, Mater. Eval. 61 (2003) 66–74.
[19] Z. Liu, C. He, B. Wu, X. Wang, S. Yang, Circumferential and longitudinal defect detection using T (0, 1) mode excited by thickness shear mode piezoelectric elements, Ultrasonics 44 (2006) 1135–1138.
[20] P. Wilcox, M. Lowe, P. Cawley, Lamb and SH wave transducer arrays for the inspection of large areas of thick plates, AIP (2000) 1049–1056.
[21] A. Kamal, V. Giurgiutiu, Shear horizontal wave excitation and reception with shear horizontal piezoelectric wafer active sensor (SH-PWAS), Smart Mater. Struct. 23 (2014) 085019.
[22] W. Zhou, H. Li, F.-G. Yuan, Fundamental understanding of wave generation and reception using d 36 type piezoelectric transducers, Ultrasonics. 57 (2015) 135–143.
[23] H. Miao, S. Dong, F. Li, Excitation of fundamental shear horizontal wave by using face-shear (d36) piezoelectric ceramics, J. Appl. Phys. 119 (2016) 174101.
[24] F. Li, H. Miao, Development of an apparent face-shear mode (d36) piezoelectric transducer for excitation and reception of shear horizontal waves via two-dimensional antiparallel poling, J. Appl. Phys. 120 (2016) 144101.
[25] Q. Huan, H. Miao, F. Li, Generation and reception of shear horizontal waves using the synthetic face-shear mode of a thickness-poled piezoelectric wafer, Ultrasonics 86 (2018) 20–27.
[26] H. Miao, Q. Huan, F. Li, Excitation and reception of pure shear horizontal waves by using face-shear d24 mode piezoelectric wafers, Smart Mater. Struct. 25 (2016) 11LT01.
[27] H. Miao, Q. Huan, Q. Wang, F. Li, Excitation and reception of single torsional wave T (0, 1) mode in pipes using face-shear d24 piezoelectric ring array, Smart Mater. Struct. 26 (2017) 025021.
[28] B. Köhler, T. Gaul, U. Lieske, F. Schubert, Shear horizontal piezoelectric fiber patch transducers (SH-PFP) for guided elastic wave applications, Ndt. E. Int. 82 (2016) 1–12.
[29] H.M. Seung, H.W. Kim, Y.Y. Kim, Development of an omni-directional shear-horizontal wave magnetostrictive patch transducer for plates, Ultrasonics 53 (2013) 1304–1308.
[30] H.M. Seung, C.I. Park, Y.Y. Kim, An omnidirectional shear-horizontal guided wave EMAT for a metallic plate, Ultrasonics 69 (2016) 58–66.
[31] Z. Liu, X. Zhong, M. Xie, X. Liu, C. He, B. Wu, Damage imaging in composite plate by using double-turn coil omnidirectional shear-horizontal wave magnetostrictive patch transducer array, Adv. Compos. Mater. 26 (2017) 67–78.
[32] C.J. Borigo, S.E. Owens, J.L. Rose, Piezoelectric shear rings for omnidirectional shear horizontal guided wave excitation and sensing, U.S. Patent 9,910,06 (2016).
[33] J.O. Kim, O.S. Kwon, Vibration characteristics of piezoelectric torsional transducers, J. Sound Vib. 264 (2003) 453–473.
[34] P. Belanger, G. Boivin, Development of a low frequency omnidirectional piezoelectric shear horizontal wave transducer, Smart Mater. Struct. 25 (2016) 045024.
[35] H. Miao, Q. Huan, Q. Wang, F. Li, A new omnidirectional shear horizontal wave transducer using face-shear (d 24) piezoelectric ring array, Ultrasonics 74 (2017) 167–173.
[36] Q. Huan, H. Miao, F. Li, A uniform-sensitivity omnidirectional shear-horizontal (SH) wave transducer based on a thickness poled, thickness-shear (d15) piezoelectric ring, Smart Mater. Struct. (2017) 08LT01.
[37] Q. Huan, H. Miao, F. Li, A variable-frequency structural health monitoring system based on omnidirectional shear horizontal wave piezoelectric transducers, Smart Mater. Struct. 27 (2018) 025008.
[38] H. Miao, F. Li, Realization of face-shear piezoelectric coefficient d36 in PZT ceramics via ferroelastic domain engineering, Appl. Phys. Lett. 107 (2015) 122902.
[39] E.V. Malyarenko, M.K. Hinders, Fan beam and double crosshole Lamb wave tomography for mapping flaws in aging aircraft structures, J. Acoust. Soc. Am. 108 (2000) 1631–1639.